JOURNAL OF MATERIALS SCIENCE **35** (2000) 3029–3035

Effect of α-SiC on the microstructure and toughening of hot-pressed SiC-AlN solid solutions

CHANG-SUNG LIM
Department of Materials Science and Engineering, Hanseo University, Seosan 356-820, Korea
E-mail: cslim@gaya.hanseo.ac.kr

The Effect of α-SiC on the microstructure and toughening of SiC-AlN solid solutions from powder mixtures of β-SiC and AlN by hot-pressing were studied in the 1870 to 2030 °C temperature range. The reaction of AlN and β-SiC(3C) powders causing transformation to the 2H(wurtzite) structure appeared to depend on hot-pressing temperatures and an additive of α-SiC. For the composition of 49 wt% AlN/49 wt% SiC with 2 wt% α-SiC and 47.5 wt% AlN/47.5 wt% SiC with 5 wt% α-SiC at 2030 °C for 1 h, the complete solid solutions with a single phase of 2H could be obtained. The appreciable amount of α-SiC could develop the columnar inter-grains of 4H phase and the stable 2H phase with the relatively uniform composition and grain size distributions. The effect of α-SiC on the phases present and compositional microstructures with columnar inter-grains was investigated using X-ray diffraction, scanning electron microscopy and transmission electron microscopy. The fracture toughness and Vickers hardness of the hot-pressed solid solutions were examined by the indentation-fracture-test method.

1. Introduction

Silicon Carbide (SiC) and aluminum nitride (AlN) have many potential applications mainly in electronic and high-temperature fields. SiC is a covalent compound which exists either in a cubic structure (3C) or in various hexagonal or rhombohedral polytypes (2H, 4H, 6H, 15R and 21R). However, there are few examples of the formation of solid solutions in the case of nonoxide ceramics with strong covalent bonds and low diffusion coefficients. The 2H polymorph of SiC is isostructural with AlN and Al_2OC with a strong covalent bond [1]. The similarities between two structures and their properties suggest that alloying of one with other may provide the potential for property optimization. During the past decade, it has been found that a series of solid solutions are formed between SiC and AlN over a wide composition range [2–23].

Cutler *et al*. [2–6] reported that a SiC-AlN solid solution in the range 2–100% AlN has been formed at 1600 °C by a vapor phase process using carbothermal reduction of amorphous silica and aluminum hydroxide in nitrogen. Ruh and Zangvil [7] described that the solid solution existed as a single phase above 2100 °C over the composition range 35–100 mol% AlN. Their flexural strengths were quite low due to inhomogeneity in grain size and composition and spinodal decomposition occurred on annealing below 1950 °C. Recently, some studies of the phase relationship and microstructures of the SiC-AlN solid solutions have been reported by hot-pressing [8–20] and pressureless sintering with additives [21–23]. In this case, the covalent bonds in SiC and AlN are strong and the diffusion coefficients are low, when all starting materials are in powder form, so that pressures of several hundred bars and temperatures of up to 2300 °C are required in order to obtain complete solid solutions with uniform composition distributions. Furthermore, its low fracture toughness of the solid solutions has to be overcome before promoting the application as engineering components.

Consequently, in this study, we focused on the effect of α-SiC as an additive on the microstructure of the complete SiC-AlN solid solutions from powder mixtures of β-SiC and AlN by hot-pressing in the 1870 to 2030 °C temperature range. Subsequently, the mechanical properties of the hot-pressed solid solutions were evaluated for hardness and fracture toughness.

2. Experimental

The materials used for this study were commercial β-SiC (Beta Randum, Ibiden Company), AlN (Grade F. Tokuyama Soda Company) and α-SiC (Du A-1 Showa Denko) powders. The major impurities in the β-SiC powder are 0.39% SiO_2, 0.64% C, 0.02% Al and 0.03% Fe, while AlN powder contains 0.89% O and 360 ppm C. The average particle sizes of the two powders are 0.27 μm and 2 μm, respectively. As an additive, α-SiC powders were used. The major impurities in the α-SiC powder are 0.46% C, 0.27% SiO_2, 0.024% Fe and 0.007% Al and the average particle size of the powder is 0.47 μm. As listed in Table I, nominal compositions investigated ranged from the composition 20 mol% AlN/80 mol% SiC (sample A20) to 90 mol% AlN/10 mol% SiC (sample A90) without the additive, and 49 wt% AlN/49 wt% SiC with the additive of 2 wt% α-SiC (sample 2W50A), 47.5 wt% AlN/47.5 wt% SiC

TABLE I Compositions and hot-pressing conditions of powder mixtures

Sample name	SiC/AlN mole ratio	Composition (wt%)			Hot-press conditions		
		SiC	AlN	α-SiC	Temp. (°C)	Time (h)	Pressure (MPa)
A20	80/20	79.6	20.4	0	1870	4	22.5
					2030	1	22.5
A50	50/50	49.5	50.5	0	1870	4	22.5
					2030	1	22.5
A70	30/70	29.6	70.4	0	1870	4	22.5
					2030	1	22.5
A90	10/90	9.8	90.2	0	1870	4	22.5
					2030	1	22.5
2W50A	50/50	49.0	49.0	2	1870	4	22.5
					2030	1	22.5
5W50A	50/50	47.5	47.5	5	1870	4	22.5
					2030	1	22.5
8W50A	50/50	46.0	46.0	8	1870	4	22.5
					2030	1	22.5

with the additive of 5 wt% α-SiC (sample 5W50A) and 46 wt% AlN/46 wt% SiC with the additive of 8 wt% α-SiC (sample 8W50A). The compositions of appropriate amounts of the powders were prepared by wet milling for 24 h in a plastic jar with isopropyl alcohol and SiC balls. After milling, the mixed powders were evaporated to dryness, broken with a mortar and passed through a 50-mesh sieve.

Specimens (3 cm in diameter by 0.5 cm thick) were uniaxially hot-pressed in graphite dies lined with graphite washer. Hot-pressing was conducted under nitrogen at 1870 °C for 4 h and at 2030 °C for 1 h under 22.5 Mpa (Table I). Cooling was sufficiently rapid, so that the high-temperature phase was quenched to room temperature. After removing the specimens from the graphite dies, the surfaces were ground. The density was determined by measuring weights and dimensions.

The ground surfaces were then polished using diamond pastes of 30, 15, 3, 1 μm. The polished specimens were ultrasonically cleaned in ethanol, rinsed with distilled water and dried. All of the specimens were examined using X-ray diffraction (XRD) with Cu K_α. The polished specimens were etched using Murakami's etch to reveal the microstructure. The etched sections were investigated using optical microscopy, scanning electron microscopy (SEM) and transmission electron microscopy (TEM). The indentation fracture test method was used with a load of 10 Kgf, a loading speed of 0.1 mm/sec and a load time of 20 sec on the finished surfaces of the specimens for measurements of fracture toughness and Vickers hardness.

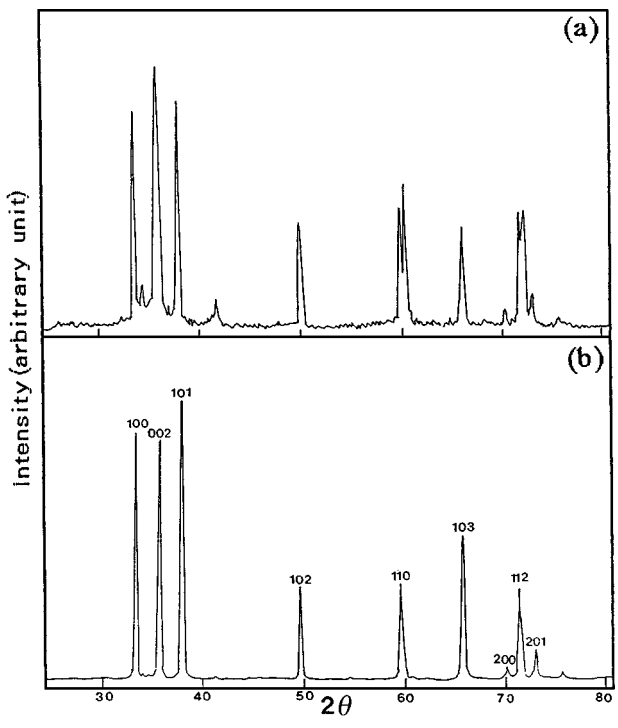

Figure 1 XRD patterns of SiC-AlN solid solutions for the sample (a) A50 and (b) 5W50A hot-pressed at 2030 °C for 1 h.

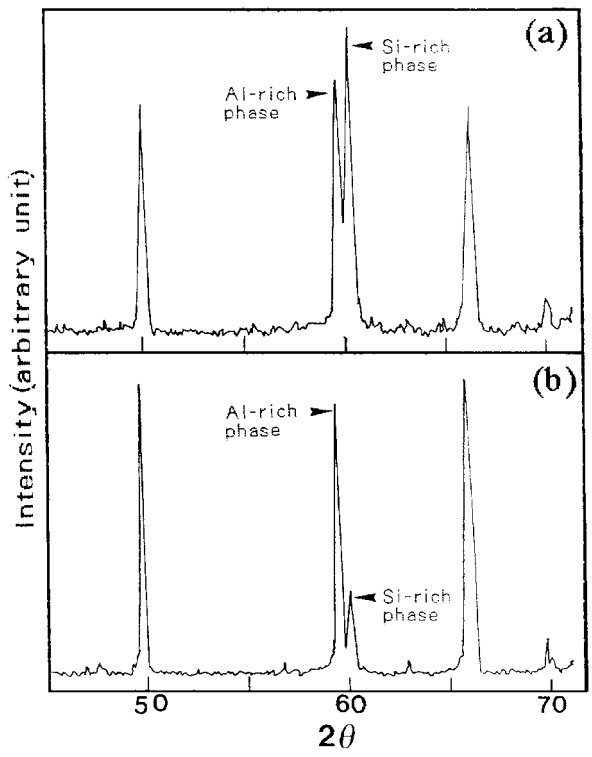

Figure 2 XRD patterns of SiC-AlN solid solutions for the sample (a) A50 and (b) A70 hot-pressed at 2030 °C for 1 h showing the typical splitting of the (110) reflection at $2\theta = 59.6°$: (a) the sample A50 indicates the splitting at $2\theta = 59.530°$ and 60.205° and (b) the sample A70 indicates the splitting at $2\theta = 59.455°$ and 60.066°, respectively.

3. Results and discussion

3.1. Phases present and phase separation behavior

As given in Table II, the phases present in the solid solutions under the various hot-press conditions were determined by XRD analysis. The phases were listed in the order of the amounts present. At 1870 °C for 4 h, for the sample A20, A50 and A70, the hexagonal 2H phase is the strongest with hexagonal 4H and 6H present and possibly some rhombohedral 15R and 3C, whereas for the sample A90 the 2H with 4H and 6H are the observed phases. At 2030 °C for 1 h, for the sample A20 the 2H phase is the strongest with 4H and 6H present and possibly some15R and 3C, while for the sample A50 and A70 the 3C phase was transformed to the hexagonal and rhombohedral phases, and for the sample A90 the 2H, 4H and 6H are present.

TABLE II Phases present in SiC-AlN solid solutions

	Hot-press conditions		
Sample name	Temp. (°C)	Time (h)	Phases present
A20	1870	4	2H, 4H, 6H, 15R, 3C
A50	1870	4	2H, 4H, 6H, 15R, 3C
A70	1870	4	2H, 4H, 6H, 15R, 3C
A90	1870	4	2H, 4H, 6H
A20	2030	1	2H, 4H, 6H, 15R, 3C
A50	2030	1	2H, 4H, 6H, 15R
A70	2030	1	2H, 4H, 6H, 15R
A90	2030	1	2H, 4H, 6H
2W50A	1870	4	2H, 4H, 6H, 15R, 3C
5W50A	1870	4	2H, 4H, 6H, 15R, 3C
8W50A	1870	4	2H, 4H, 6H, 15R, 3C
2W50A	2030	1	2H
5W50A	2030	1	2H
8W50A	2030	1	2H, 4H

Results for the sample 2W50A, 5W50A and 8W50A at 1870 °C for 4 h were similar to the result for the sample A50 at 1870 °C for 4 h. On the other hand, when these compositions were hot-pressed at 2030 °C for 1 h, a single solid solution of 2H was obtained for the sample 2W50A and 5W50A and 2H with some 4H for the sample 8W50A. These results indicate that the reaction of AlN and β-SiC powders causing the transformation to the 2H phase appeared to depend on the hot-pressing temperatures and the additives of α-SiC present.

Typical XRD patterns on the sample A50 and 5W50A at 2030 °C for 1 h are shown in Fig. 1. The hexagonal lines with various splittings on the sample A50 in Fig. 1a indicate the 2H solid solution with various polytypes, whereas the strong hexagonal lines with the absence of any splitting indicate that the sample 5W50A is a single solid solution of 2 H in Fig. 1b. For this solid solution, the 2θ value for the (100) reflection is 33.3°, while that for AlN would be 33.2° and that for SiC (2H) would be 33.7°.

Fig. 2 shows the typical splitting of the (110) reflection of the sample A50 and A70 at 2030 °C for 1 h. Fig. 2a for the sample A50 shows the typical splitting at $2\theta = 59.530°$ and 60.205°, which indicates the high intensity value of a Si-rich phase. On the other

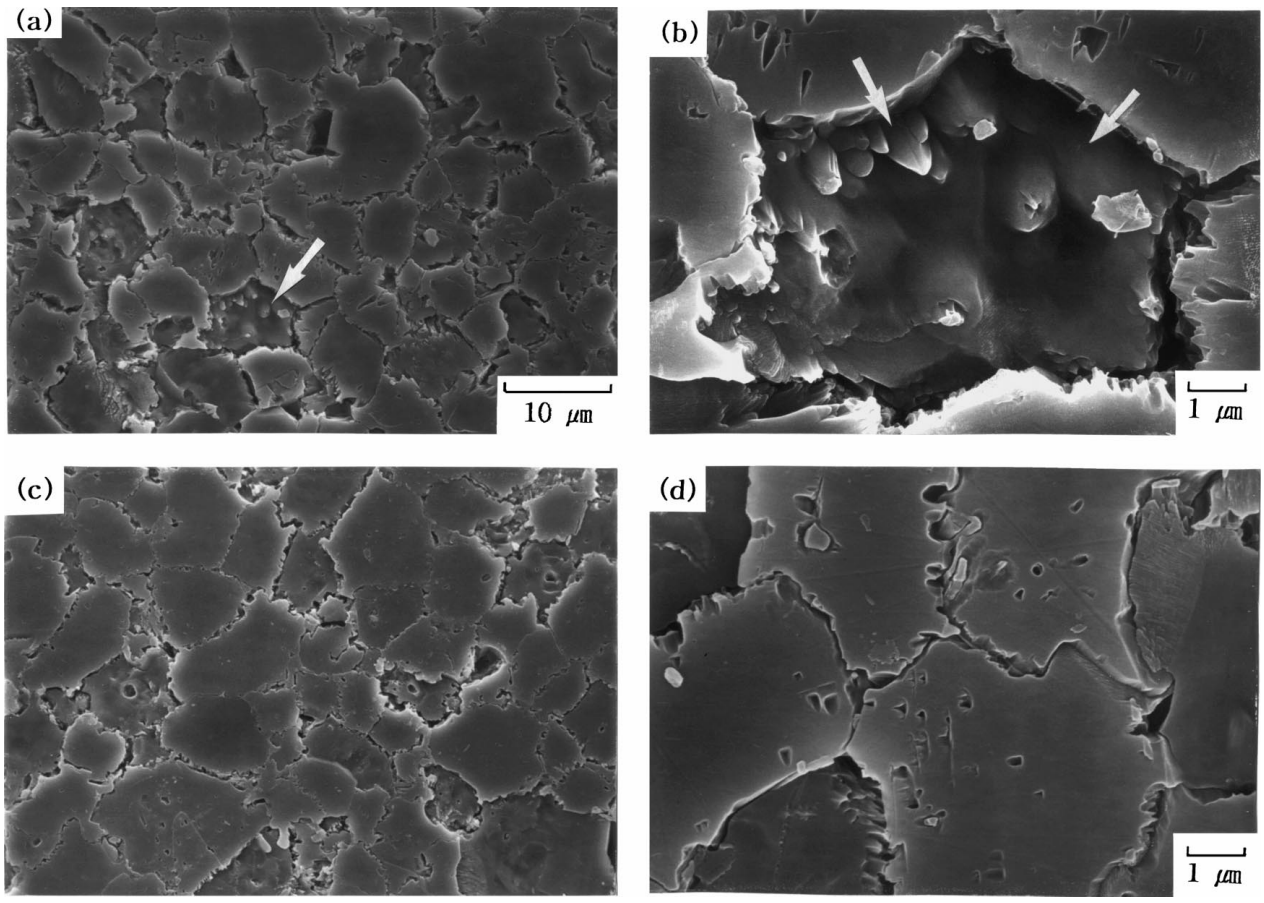

Figure 3 Scanning electron micrographs and high magnifications of SiC-AlN solid solutions for the sample 2W50A ((a) and (b)) and 5W50A ((c) and (d)) as hot-pressed at 2030 °C for 1 h. The arrow of (a) and (b) indicates the small amount of columnar inter-grains.

hand, Fig. 2b for the sample A70 shows the splitting at $2\theta = 59.455^\circ$ and 60.066°, which indicates the high intensity value of an Al-rich phase. The crystalline of the SiC-AlN solid solutions consisted of two main phases: one was the SiC-rich solid solution phase and another was the AlN-rich solid solution phase [9, 14]. The (110) reflection of the SiC-AlN solid solution provides the maximum possibility of observing splitting with the two phases of identical structure due to slightly different lattice parameters. It had the largest 2θ difference between SiC and AlN of the major diffraction peaks. This phase separation was presumed to be of spinodal or binodal decomposition, considering the peak splitting behavior [13–15, 20].

3.2. Microstructural evolution with columnar inter-grains

Results of SEM studies were good agreement with XRD results. Figs 3 and 4 show typical microstructures of the SiC-AlN solid solutions for the sample 2W50A, 5W50A and 8W50A as hot-pressed at 2030 °C for 1 h, which previously were etched using Murakami's etch. All of the samples had densities in excess of 99% of theoretical density. According to the XRD results, for the composition of 49% AlN/49% SiC with an additive of 2 wt% α-SiC (2W50A) or 47.5% AlN/47.5% SiC with an additive of 5 wt% α-SiC(5W50A), the complete solid solutions with a single phase of 2H was obtained by hot pressing at 2030 °C for 1 h. The microstructures of the sample 2W50A and 5W50A in Fig. 3 show relatively uniform grain size distributions. The sample 2W50A exhibits a small amount of columnar inter-grains in the grain by the arrow in Fig. 3a and b. In contrast, the sample 8W50A exhibits an inhomogeneous size distribution and a large proportion of heavy strained and faulted grains in Fig. 4a and with exaggerated columnar inter-grains in complicated grain mixtures in Fig. 4b, which suggest either untransformed or in the process of the transformation from 4H to 2H.

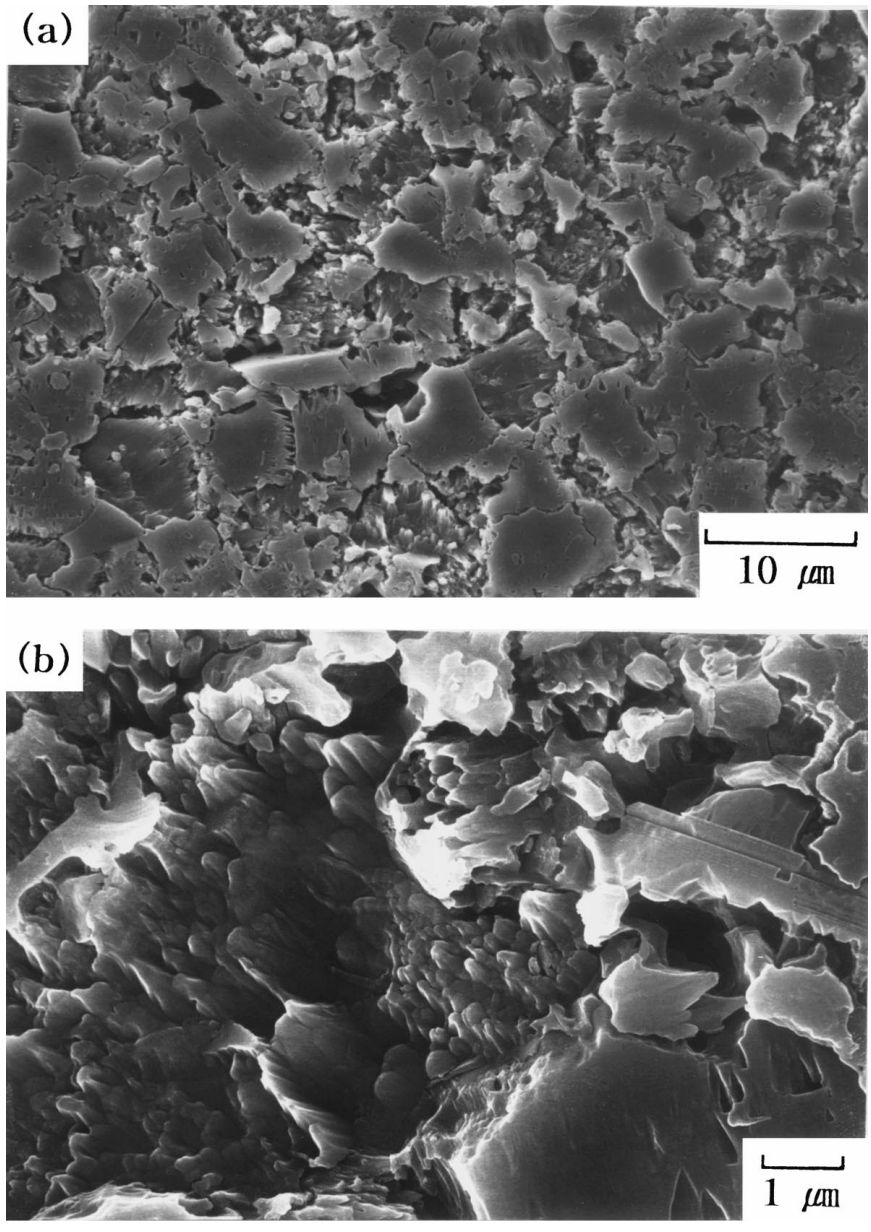

Figure 4 Scanning electron micrograph (a) and high magnification (b) of SiC-AlN solid solution for the sample 8W50A as hot-pressed at 2030 °C for 1 h.

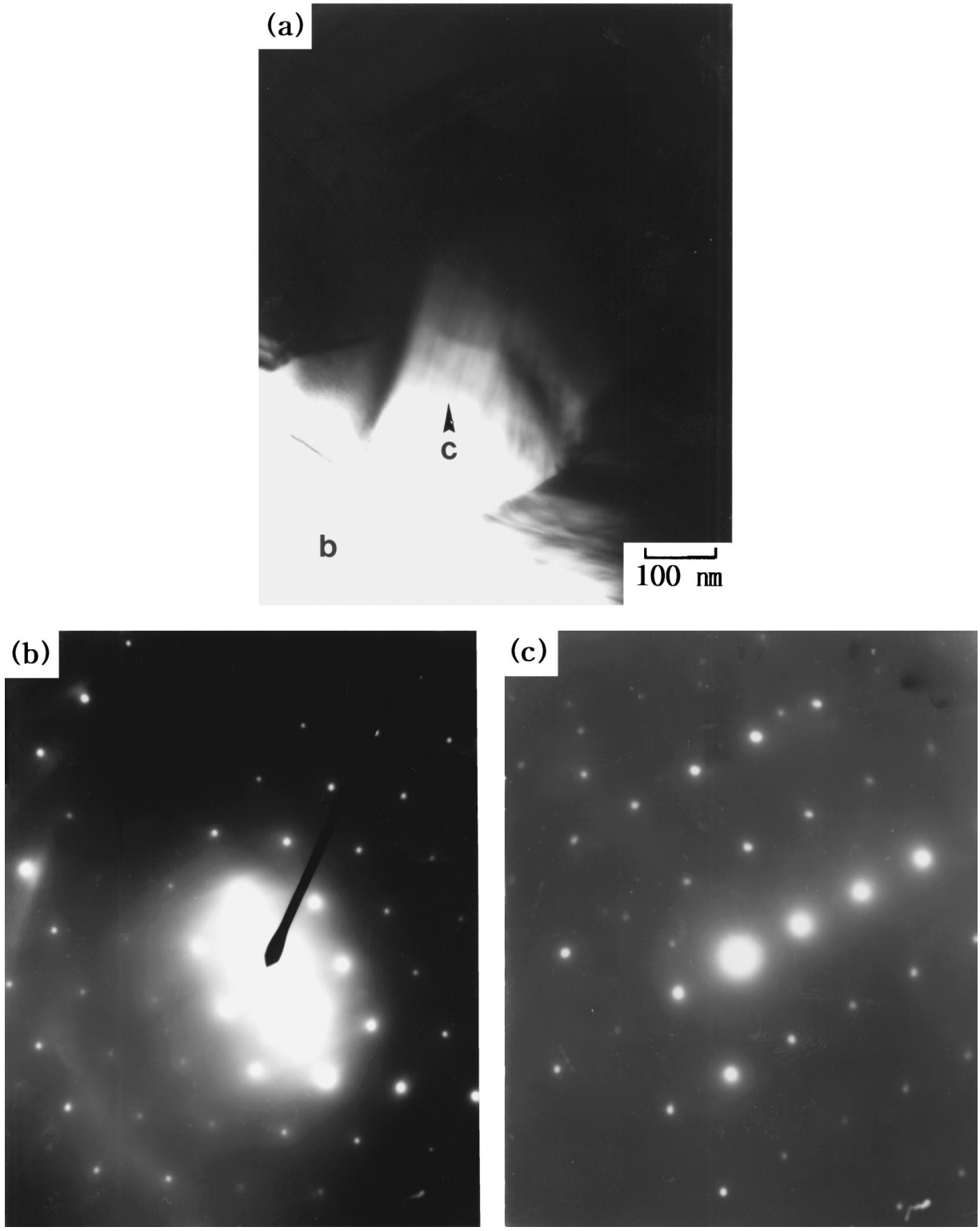

Figure 5 Transmission electron micrograph (a) and diffraction patterns of 2H phase (b) and 4H phase (c) in SiC-AlN solid solutions.

Fig. 5 shows a TEM micrograph (a) and diffraction patterns ((b) and (c)) of the columnar inter-grain in the 2H phases. The columnar inter-grain was identified to be 4H (Fig. 5c) and the surrounded phase to be 2H (Fig. 5b). Therefore, it is noted that the appreciable amount of α-SiC could develop the columnar inter-grains of 4H phase and the stable 2H phase with the uniform composition and grain size distributions.

3.3. Tentative phase diagram

Fig. 6 shows a tentative SiC-AlN phase diagram [14]. For the pure-SiC axis of the diagram, it is assumed that the sequence of stable polytypes with increasing temperature is β, 2H, 4H, 6H. This sequence is not clearly observed experimentally because of the very close thermodynamic stability of the polytypes. The mixture of hexagonal polytypes was observed between

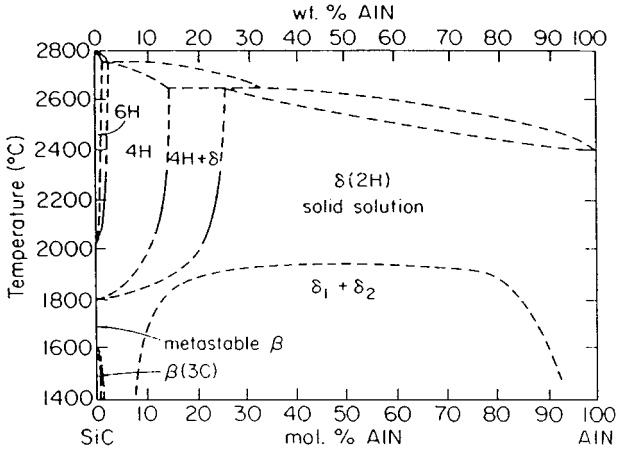

Figure 6 Tentative SiC-AlN phase diagram [14].

1870 °C and 2030 °C temperature range in this study. It could be assumed that the the AlN and β-SiC transformed to β-2H, 6H-4H and 4H-2H. The metastable β phase is shown above1600 °C and may extend to around 2000 °C. Above 2000 °C a single solid solution (designated δ) with the 2H structure and 2H + 4H two phase are observed from 23% AlN to 100% AlN. The miscibility gap has been suggested by Rafaniello *et al.* [9] who conducted annealing experiments of solid solutions obtained by carbothermal reduction reaction. They found that the solid solutions, which were obtained at low temperatures, were metastable and tended to separate to SiC-rich and AlN-rich phases, denoted here as δ_1 and δ_2, respectively. The SiC-rich and AlN-rich phases were also observed in the sample A50 and A70 hot-pressed at 2030 °C for 1 h in Fig. 2. It seems certain that the location of the miscibility gap and the other phase boundaries in the diagram are dependent on the raw materials, additives and pressures. It was considered that the α-SiC content of the reaction of AlN and β-SiC affected the SiC-AlN phase relationships and the microstructures by stabilizing the 2H phase. The appreciable amount of α-SiC could develop the stable 2H phase with the columnar inter-grains of 4H phase at 2030 °C.

3.4. Mechanical properties

Table III shows results from the fracture toughness and Vickers hardness measurements for the SiC-AlN solid solutions. The sample 5W50A was 5.4 MPa·m$^{1/2}$ and the sample 2W50A and 8W50A were 5.3 and 5.1 MPa·m$^{1/2}$, respectively. These values of the fracture toughness are higher than other works [17, 21, 23] in the SiC-AlN solid solutions, which presented the values ranged between 3.7 and 4.6 MPa·m$^{1/2}$. The enhanced fracture toughness of this study is due to the reinforcement of the columnar inter-grains of 4H phase in the 2H phase by the appreciable amount of α-SiC. The average hardness on the sample 2W50A, 5W50A and 8W50A shows the value of 16.7 and 18.8 GPa, which shows no difference comparing with other work [23].

TABLE III Fracture toughness and Vickers hardness of SiC-AlN solid solutions hot-pressed at 2030 °C for 1 h

Sample name	Fracture toughness (MPa·m$^{1/2}$)	Vickers hardness (GPa)
2W50A	5.29 ± 1.23	17.09 ± 0.15
5W50A	5.43 ± 1.11	18.81 ± 0.12
8W50A	5.05 ± 1.54	16.68 ± 1.34

4. Conclusions

The effect of α-SiC on the microstructure and toughening of SiC-AlN solid solutions prepared from powder mixtures of AlN and β-SiC by hot-pressing was investigated in the 1870 °C to 2030 °C temperature range. The reaction of AlN and β-SiC powders causing transformation to the 2H structure appeared to depend on the hot-pressing temperatures and additives of α-SiC present. The crystalline of the SiC-AlN solid solutions consisted of a SiC-rich solid solution phase and an AlN-rich solid solution phase. For the composition of 49 wt% AlN/49 wt% SiC with 2 wt% α-SiC (2W50A) and 47.5 wt% AlN/47.5 wt% SiC with 5 wt% α-SiC (5W50A) at 2030 °C for 1 h, the complete solid solutions with a single phase of 2H could be obtained. The appreciable amount of α-SiC could develop the columnar inter-grains of 4H phase and the stable 2H phase with the relatively uniform composition and grain size distributions. The fracture toughness of the sample 5W50A was 5.4 MPa·m$^{1/2}$ and the sample 2W50A and 8W50A were 5.3 and 5.1 MPa·m$^{1/2}$, respectively, which are higher than other works in SiC-AlN solid solutions. The enhanced fracture toughness is due to the reinforcement of the columnar inter-grains of 4H phase in the 2H phase induced by the appreciable amount of α-SiC.

Acknowledgement

This work was supported by the Korea Science and Engineering Foundation (KOSEF) under contract No. 961-0802-014-2.

References

1. D. BLOOR, R. J. BROOK, M. C. FLEMINGS, S. MAHAJAN and R. W. CAHN, "The Encyclopedia of Advanced Materials," Vol. 4 (1995) p. 2453.
2. I. B. CUTLER, P. D. MILLER, W. RAFANIELLO, H. K. PARK, D. P. THOMSON and K. H. JACK, *Nature* **275** (1987) 795.
3. W. RAFANIELLO, K. CHO and A. V. VIRKAR, *J. Mat. Sci.* **16** (1981) 3479.
4. Y. SUGAHARA, K. I. SUGIMOTO, H. TAKAGI, K. KURODA and C. KATO, *J. Mat. Sci. Lett.* **7** (1988) 795.
5. K. TSUKUMA, M. SHIMADE and M. KOIZUMI, *ibid.* **1** (1982) 9.
6. Y. SUGAHARA, K. KURODA and C. KATO, *J. Amer. Ceram. Soc.* **69** (1984) C247.
7. R. RUH and A. ZANGVIL, *ibid.* **65** (1982) 260.
8. L. D. BENTSEN, D. P. H. HASSELMAN and R. RUH, *ibid.* **66** (1983) C40.
9. W. RAFANIELLO, M. R. PLICHTA and A. V. VIRKAR, *ibid.* **66** (1983) 272.
10. A. ZANGVIL and R. RUH, *Mat. Sci. Eng.* **71** (1985) 159.
11. R. RUH, A. ZANGVIL and J. BARLOWE, *J. Amer. Ceram. Soc. Bull.* **64** (1985) 1368.

12. Z. C. JOU, S. Y. KUO and A. V. VIRKAR, *J. Amer. Ceram. Soc.* **69** (1986) C279.
13. S. Y. KUO, A. V. VIRKAR and W. RAFANIELLO, *ibid.* **70** (1987) C125.
14. A. ZANGVIL and R. RUH, *ibid.* **71** (1988) 884.
15. S. Y. KUO and A. V. VIRKAR, *J. Amer. Ceram. Soc.* **73** (1990) 2640.
16. I. TEUSEL and C. RUSSEL, *J. Mat. Sci.* **25** (1990) 3531.
17. J. F. LI and R. WATANABE, *ibid.* **26** (1991) 4813.
18. Y. XU, A. ZANGVIL, M. LANDON and F. THEVENOT, *J. Amer. Ceram. Soc.* **75** (1992) 325.
19. R. SATHYAMOORTHY, A. V. VIRKAR and R. A. CUTLER, *ibid.* **75** (1992) 1136.
20. J. CHEN, Q. TIAN and A. V. VIRKAR, *ibid.* **75** (1992) 809.
21. R. R. LEE and W. C. WEI, *Ceram. Eng. Sci. Proc.* **11** (1990) 1094.
22. I. TEUSEL and C. RUSSEL, *J. Mat. Sci. Lett.* **11** (1992) 205.
23. M. MIURA, T. YOGO and S. I. HIRANO, *J. Mat. Sci.* **28** (1993) 3859.

Received 22 April
and accepted 13 December 1999